



COVER SHEET

Adam, Clayton and Pearcy, Mark and McCombe, Peter (2003) Stress analysis of interbody fusion – finite element modelling of inter-vertebral implant and vertebral body. *Clinical Biomechanics* 18:pp. 265-272.

Copyright 2003 Elsevier

Accessed from: <https://eprints.qut.edu.au/secure/00003712/01/paper1.pdf>

Stress analysis of interbody fusion – finite element modelling of inter-vertebral implant and vertebral body

Clayton Adam¹, PhD, Mark Pearcy¹, PhD, Peter McCombe², MB.BS., FRACS

¹School of Mechanical, Manufacturing and Medical Engineering, Queensland University of Technology, Brisbane, Australia,

²Brisbane, Australia

Name and address for correspondence

Dr Clayton Adam

Lecturer in Mechanics/Design

School of Mechanical, Manufacturing and Medical Engineering

Queensland University of Technology

GPO Box 2434, 2 George St, Brisbane Q4001 AUSTRALIA

Phone +61 7 3864 2638

Fax +61 7 3864 1469

Email c.adam@qut.edu.au

Sources of support

This research was partially supported by Medtronic Sofamor Danek

Abstract

Objective: To investigate stresses in interbody fusion systems during compressive loading.

Design: The study uses finite element methods to investigate predicted stresses. Previously published experimental material properties are used as inputs to the numerical simulation.

Background: Interbody spinal fusion procedures using cage style inter-vertebral implants often cause subsidence failure of the vertebral end plate, resulting in potential pain and mechanical instability of the fusion system.

Methods: Finite element models were developed to simulate compressive load transfer between interbody implants and adjacent vertebral body. The vertebral body was modelled using tied finite element mesh regions for cancellous core and cortical shell, and non-linear frictional contact between implants and vertebral end plate.

Results: Simulation results predicted end plate stresses of approximately twelve times the nominal contact pressure due to differing deformation stiffnesses of the implant and end plate structures. Reduction of the cancellous core elastic modulus to simulate severely osteoporotic bone resulted in end plate stresses up to three times higher than the benchmark values.

Conclusions: In this study, finite element analysis was used to investigate the stresses in interbody fusion systems. Published vertebral loads corresponding to certain activities were shown to generate end-plate stresses which approach and exceed the failure stress for cortical bone.

Relevance

End-plate subsidence failure can potentially occur at the corners of existing cage-type interbody implants under physiological compressive loads. Matching material properties between cortical end-plate and implant does not guarantee optimal contact conditions, and overall bending stiffness should be assessed.

Keywords

Spinal fusion, interbody fusion implant, finite element, stress analysis, back pain, vertebrae

Introduction

Interbody fusions using an inter-vertebral implant of the 'cage' design have become increasingly common in the field of spinal surgery in recent years. Commercially available implants come in many designs and are constructed from a variety of materials, though all function as load-carrying members to provide stability in the three to six months between inter-vertebral disc removal and subsequent biological formation of a full thickness bone bridge. In order to promote bone growth, the implants are usually designed as hollow spacers to accommodate internal packing of cancellous bone graft. The implants maintain vertebral body separation while the cancellous graft slowly forms a mass of new bone.

To function as primary load-bearing structures, spinal fusion implants must be capable of withstanding the loads applied to them in vivo during post operative patient activity. This requirement for structural integrity is readily met with the use of high strength materials and adequate geometric dimensions (such as implant wall thickness). However, the introduction of relatively small surface area, rigid implants into a space which was previously occupied by a high compliance, high surface area inter-vertebral disc significantly changes the pattern of stress distribution on the adjacent vertebral bodies, particularly on the vertebral end plates. As a result, subsidence failure of the vertebral end plate due to implant penetration is a common clinical finding. Kuslich [2] showed in a series of surgical procedures to remove herniated inter-vertebral discs under local anaesthetic that the vertebral end plate was a potent source of pain when probed in some (but not all) patients. Failure of the end plate due to implant penetration is therefore a potential source of post operative pain in fusion patients.

In an experimental investigation of vertebral body failure under implant loading, Pearcy [6] showed that with full thickness tri-cortical iliac autografts, subsidence failure into the

vertebral body under load was common if the combined surface area of contact of the grafts was less than 40% of the surface area of the vertebral end plate. Such findings indicate that the geometry, material properties, and loading configuration of implants and vertebral bodies are important determinants of the resulting stress distribution. Excessively high stresses can lead to end plate subsidence failure and mechanical instability of the attempted fusion.

Several authors [1,4] have created finite element models of the vertebral body and/or inter-vertebral disc under compressive loading. Previous finite element investigation of thread style fusion implants has also been published [7]. This study presents detailed finite element simulation of the contact and internal stresses generated by compressive loading of laproscopic cage type implants against an adjacent vertebral body. A benchmark three-dimensional finite element model was developed to simulate load transfer between a 'generic' implant geometry and an anatomically simplified vertebral body consisting of external cortical shell and cancellous interior. The finite element model was used to predict stress, strain, and deformation levels in each component at a given compressive load, and to determine the loads at which end plate subsidence failure was likely to occur. Numerical sensitivity analyses were then performed to compare stress levels for a range of material properties with those of the benchmark model. The applicability of the finite element methodology for assessment of different implant designs, material properties, and loading conditions was demonstrated.

Methodology

A 'generic' implant of the hollow cage design was used in the current investigation to provide a general picture of the load transfer mechanisms and resultant end plate stresses associated

with this type of implant. The three dimensional finite element model consists of two such implants contacting a geometrically simplified vertebral body.

Component Geometry

The generic implant was of similar external dimensions to commercially available devices (10×12×25mm), but with simplified geometry. Each contact surface was flat and smooth with a surface area of 152mm². The hollow space inside the implant was a filleted 6×19mm rectangle with contact surface area of 106mm². External edges were filleted with a 0.5mm radius to reduce edge stress concentrations at the contact interface.

The vertebral body was idealised as a 1.0mm thick cortical outer shell¹, with an internal cancellous core. The finite element meshes for the cancellous core and cortical shell were tied together, simulating the biological connection between the two materials. Symmetry considerations were used to model only the upper portion of the vertebral body. The end plate was assumed flat in the current model, and the transverse section of the vertebral body was a reproduction of the actual vertebral body geometry of an L5 vertebra. The cortical side walls were assumed smooth and vertical, and joined the end plate via a 2.0mm transition fillet radius.

The benchmark model comprised the two implants, the cortical outer shell, and the cancellous interior core of the vertebral body. The simulation did not include bone graft inside the implant ‘cages’ of the benchmark model.

¹ Which lies within the thickness range of 0.4-1.3mm reported in [4].

Loads and Boundary Conditions

Given the (approximate) symmetry of the interbody space, only one vertebral body was modelled, and the desired compressive load was then applied directly to the non-contacting upper faces of the implants. The vertebral body half-model was fully constrained at its base, and the load transmitted through the model was therefore supported partially by the cancellous core and partially by the cortical shell side walls. For the benchmark case, a total load of 610N (simulating an individual with a body weight of 62kg) was applied to the upper surfaces of the implants as a uniformly distributed pressure. This nominal load was similar in magnitude to the ‘normal standing load’ of 700N (71kg) reported in [8]. However, the actual magnitude of applied load is not critical in the present analysis since as a first approximation the results may be assumed scalable².

Contact and Friction

A Coulomb friction contact algorithm was used to model the normal and frictional force transmission between implants and vertebral end plate. The coefficient of friction for the interaction was set to 0.3 for the benchmark case, and this value was varied to investigate the effect of friction coefficient on predicted stresses. Commercially available implants often have serrated contact surfaces, creating higher effective friction coefficients than would be expected with smooth contacting surfaces.

Material Properties

² The contact interaction between implants and end plate introduces a non-linearity into the numerical solution due to the changing contact ‘footprint’ and potential for frictional sliding, however for the present study stresses were assumed linear with load to approximately determine failure loads.

Isotropic linear elasticity was used to describe the constitutive behaviour of all components in the finite element model. The required properties for each material were therefore the elastic modulus (E) and Poisson's ratio (ν). The compressive elastic modulus for implant materials varies widely; $E \approx 1.3$ GPa for softer non-metallic compounds such as PEEK³, $E = 6.5$ GPa for a typical carbon reinforced polymer, $E \approx 115$ GPa for Titanium, and $E \approx 160$ GPa for Stainless Steel. For the benchmark case, a value of $E = 6.5$ GPa was used. Poisson's ratio for these implant materials is consistently in the range $\nu = 0.2-0.3$, and a value of 0.2 was used for the benchmark case.

Elastic properties for cortical and cancellous bone are less well defined and more subject to natural variation. Bone exhibits significant anisotropy, and so any attempt at modelling with isotropic constitutive properties is an approximation to the complexities of the real material. In the current study, a compressive Young's modulus $E = 5$ GPa was used for cortical bone, corresponding to the lower end of the 5-28 GPa cortical elastic modulus range reported by Nigg and Herzog [5]. Linde [3] reports measurements varying between $E = 20$ MPa and $E = 1080$ MPa for trabecular (cancellous) bone. A value of $E = 74$ MPa was used for cancellous bone in the benchmark case [1]. Poisson's ratio for both cancellous and cortical bone was equated to 0.2, although there is some evidence to suggest that Poisson's ratio for cancellous bone may be 0.1 or even lower [3].

While the linear elasticity models do not implicitly simulate material failure at high stress levels, the likelihood of material failure may be assessed by comparison with known failure stress levels. Linde [3] suggests a failure stress level of 4 MPa for Cancellous bone. Nigg and Herzog [5] quote failure stresses for cortical bone (femur) in the range 131-224 MPa for

³ PolyEthylEthylKetone

compression, and 80-150MPa for tension. Taking the conservative lower end of these ranges, we assumed failure stresses of 80MPa and 130MPa for tension and compression of cortical bone respectively. The failure stresses for implant materials are generally high (>100MPa) and end plate subsidence failure is usually the primary mode of damage, rather than failure of the implant itself.

Meshing

All model components were discretized using a tetrahedral finite element mesh. The 1.0mm thickness cortical shell required a small (<1mm) element size for discretization of this region. Note that the adequacy of tetrahedral elements under bending-dominated stress states (as may occur in the vertebral end plate) is strongly dependent on mesh size and problem geometry, and the existing model mesh will be assessed with regard to numerical accuracy in future studies. For the purposes of the current study however, the model mesh provided a satisfactory comparative tool. Figure 1 shows the assembled model and finite element mesh with the position of loads, boundary conditions, and frictional interaction indicated. The model was solved using the ABAQUS/Standard finite element software.

Results and Discussion

Benchmark Simulation

A benchmark simulation was performed to demonstrate the finite element methodology, predict typical stress distributions within the system, and to provide a reference for studying the effects of various model parameters using sensitivity analysis. Previously discussed material properties and simulation conditions were used for the benchmark finite element simulation.

Figure 2 shows the predicted von Mises stress⁴ distribution in the benchmark finite element model (with one implant removed to show end plate stresses more clearly). An important observation is the uneven stress distribution beneath the contacting faces of each implant. Rather than distributing the applied load evenly, the implants tend to deform the vertebral end plate such that each implant is supported largely by its outer corners and anterior/posterior edges. This deformation pattern results in high end plate stresses (maximum von Mises stress of 25.0MPa) underneath the corners of the implant. Given this non-uniform contact pressure distribution, the presence of internal bone graft in the cage would initially have little effect on stress levels since the majority of compressive load is being transmitted through the edges of the implant, with little (if any) contact adjacent to the hollow central region.

For this loading case, a simple ‘nominal’ contact stress can be calculated as $\sigma = F/A = 2.0$ MPa (assuming full-face contact, where $A=152\text{mm}^2$ and $F=305\text{N}$ per implant). Comparison with the 25MPa maximum von Mises stress in Figure 2 shows that the predicted maximum stress for the model was approximately twelve times higher than the ‘nominal’ contact stress.

Figure 3 shows the predicted von Mises stresses in one of the implants. The maximum implant stress of 15MPa for this case is approximately 40% lower than the maximum end plate stress of 25MPa. As expected, the high stress locations in the implant (anterior and posterior edges) correspond to the high stress locations on the adjacent vertebral end plate.

⁴ von Mises stress is a commonly used invariant stress measure which considers all of the normal and shear stress components acting at some location in the material. Critical von Mises stress values are often used to define the onset of failure for ductile materials.

The predicted stress levels in the cancellous core are much lower than those in the cortical shell, with a maximum value of 0.75MPa. These lower stress levels are due firstly to the low elastic modulus of cancellous bone compared to cortical bone, and secondly to the direct compressive load application that the cancellous core experiences, as opposed to the indirectly induced bending loads in the cortical shell. The cancellous core plays an important role in supporting the vertebral end plate under compressive loading. This function is discussed further in the next section.

These results suggest that in reality, further end plate subsidence adjacent to the edges of the implant would need to occur before the interior regions of the implant (including the bone graft) contacted the end plate and were able to share compressive load. Also, a more anatomically realistic concave end plate would tend to exacerbate this situation, edge subsidence failure of several millimetres may be necessary before the full implant contact area and bone graft play any significant role in the load transfer mechanism between implant and end plate. Figure 4 shows an amplified view of the deformed end plate, with all deformations magnified 100 times. The amplified surface profile clearly shows the punch-like indentations adjacent to the implant edges, and essentially unloaded region closer to the interior. Table 1 summarises the stress results from the benchmark simulation.

Comparison of these predicted maximum stress levels with the failure stresses for cortical bone mentioned previously suggests that a load of 3.2 times the benchmark load, or 1952N could be applied before a von Mises stress of 80MPa was reached⁵. Alternatively, if failure was defined by comparison with tensile principal stress only, then a load of 5.2 times the benchmark value, or 3172N could be applied before a tensile principle stress of 80MPa was

⁵ Note that these observations assume linear scalability of the finite element results (refer footnote 2).

reached. By comparison, White and Panjabi [7] report measured loads in the third lumbar disc of up to 3400N for heavy lifting conditions with back bent. Loads of 1200N were reported for activities such as laughing or bending forward, while loads of 1800N were reported for sit-up exercises with knees bent. Comparison of these measured load levels with the finite element predicted failure loads suggests that even with an idealised flat end plate, low modulus implant, and healthy cancellous vertebral core, failure stress levels could conceivably be reached when performing certain strenuous activities.

Parameter Variation – Sensitivity Analysis

Having examined the predicted stress levels and load distribution patterns for the benchmark case, a sensitivity analysis was performed to investigate the effects of varying certain model parameters on predicted maximum stress levels within the model. These results were generated by repeated finite element simulation with different values of the parameter in question, varying one parameter at a time.

Figure 5 shows the effect of the cancellous bone elastic modulus on three measures of maximum predicted stress; von Mises, principal tensile, and principal compressive. This graph demonstrates the significant dependence of end plate stress on the cancellous core elastic modulus, especially for core modulus values less than 100MPa. The decreasing ability of ‘softer’ core material to support the end plate causes rapidly increasing cortical stresses, up to a maximum von Mises stress value of 75MPa for a totally porotic core ($E \Rightarrow 0$). This stress is three times higher than the 25MPa maximum stress for the benchmark simulation at the same load, suggesting that end plate failure could occur at much lower loads if the cancellous core elastic modulus is low (for example in patients with osteoporosis).

Figure 6 shows the predicted proportion of total load carried by the cancellous core versus the core elastic modulus. At the benchmark modulus ($E=74\text{MPa}$), 36% of total compressive load is transmitted through the cancellous core, and the other 64% through the cortical shell sidewalls. By comparison, White and Panjabi [8] report measurements in which the cancellous core was found to carry 35% of load after age 40, having decreased from 55% of total load before age 40.

Sensitivity analysis was also performed to investigate the variation of predicted maximum stresses with the implant elastic modulus over the range $E=1.3\text{GPa}$ to $E=200\text{GPa}$. The resulting variation is shown in Figure 7. Maximum von Mises stress increased by 46% from 19.2MPa (for a compliant $E=1.3\text{GPa}$ material), to 28.1MPa (for a very rigid $E=200\text{GPa}$ implant). The graph in Figure 7 displays a distinct knee below $E=5\text{GPa}$, with more compliant materials reducing maximum stress levels. However, the use of compliant materials raises other questions regarding the implant's ability to resist compressive deformation and maintain constant inter-vertebral space so that rigid bony fusion can occur. Although the elastic modulus of the implant affects stress levels, the variation is much less than would be expected based on a linear variation of maximum stress with implant elastic modulus. This issue is discussed further in the next section.

The friction coefficient between implant and vertebral end-plate also has some effect on maximum stresses, with a predicted 22% increase in von Mises stress (from 21.8MPa to 26.5MPa) when varying the friction coefficient between 0.1 and 0.5. Values of friction coefficient higher than 0.5 had no further effect on maximum stress, indicating that any potential tangential motion at the contact interface had been completely constrained. Although a low friction contact interface may reduce stresses, practical considerations of implant

stability and immobility would appear to warrant the use of implants which grip the vertebral end plate adequately.

Beam Bending Stiffness Analogy

Little attention has previously been paid to the difference in elastic bending stiffness between implants and vertebral end plate. In the past, implants constructed from low elastic modulus materials have been praised because the modulus of elasticity is similar to that of cortical bone. However, the elastic bending stiffness of a structural member should not be confused with the elastic modulus, since the elastic bending stiffness is determined by geometry as well as by elastic material properties. Using engineering beam bending theory, elastic bending stiffness is defined as the product of the elastic modulus (E) and the area moment of inertia for the beam cross section (I)⁶. If the present low modulus ($E=6.5\text{GPa}$) 'generic' implants and the vertebral end plate ($E=5.0\text{GPa}$) are idealised as elastic beams supported at the anterior and posterior edges of the vertebral end plate, the elastic bending stiffnesses (EI) for each structure can be estimated as shown schematically in Figure 8.

Figure 8 shows that although the elastic moduli of the two materials are similar, the bending stiffness of the implants ($EI=6.5\text{Nm}^2$) is 300 times greater than that of the idealised end plate ($EI=0.021\text{Nm}^2$). This analogy helps to explain the markedly different deformation responses between the two structures that resulted in high stresses at the contacting edges. In designing implants for improved end plate stress distribution, comparison of deformation characteristics between implants and end plate should be made on the basis of bending stiffness, EI , rather than purely on elastic modulus, E . The implant surface area will also be an important determinant of stress levels, but the current analysis suggests that high edge loadings will

⁶ The area moment of inertia for a rectangular beam cross-section of depth d and width b is defined as $I=bd^3/12$.

cause premature local material failure and implant subsidence before the full implant surface area (and internal bone graft) is able to contact the end plate and begin sharing load.

Conclusions

This paper presents a finite element model of a generic inter-vertebral implant and anatomically simplified vertebral body for the simulation of post operative compressive loading of the surgical fusion system. Using accepted values for material constants, the implant induces stresses up to twelve times higher than the nominal contact pressure in the vertebral end plate adjacent to its anterior and posterior edges. These stresses may approach or exceed cortical bone failure levels during some activities. The simulation results demonstrate the applicability of finite element methods to this class of problem.

Sensitivity analysis was used to quantify the significant role of the cancellous core in load-sharing and end plate support. End-plate stresses increased by a factor of three for a porous cancellous core. The sensitivity analysis also predicted clinically important variations of maximum stress with implant elastic modulus.

The study highlights the necessity to consider overall elastic bending stiffness (implant geometry and elastic modulus) rather than just elastic material properties when assessing implant to end plate load transfer.

Acknowledgements

The authors wish to express their thanks to Medtronic Sofamor Danek for contributing to this work.

References

- 1 Belytschko T, Kulak RF, Schultz AB. Finite element stress analysis of an inter-vertebral disc. *Journal of Biomechanics*, 1974;7(277).
- 2 Kuslich S, Ulstrom C, Michael CJ. The tissue origin of low back pain and sciatica: A report of pain response to tissue stimulation during operations on the lumbar spine using local anesthesia. *Orthopedic Clinics of North America*, 1991;22(2):181-187.
- 3 Linde F. Elastic and viscoelastic properties of trabecular bone by a compression testing approach. *Danish Medical Bulletin*, 1994;41(2).
- 4 Mizrahi J, Silve MJ, Keaveny TM, Edwards WT, Hayes WC. Finite-element stress analysis of the normal and osteoporotic lumbar vertebral body. *Spine*, 1993;18(14).
- 5 Nigg BM, Herzog WH (Eds). *Biomechanics of the musculo-skeletal system*. John Wiley & Sons, Chichester, 1994.
- 6 Pearcy MJ, Evans JH, O'Brien JP. The load bearing capacity of vertebral cancellous bone in interbody fusion of the lumbar spine. *Engineering in Medicine*, 1983;12:183-184.
- 7 Kim Y. Prediction of mechanical behaviors at interfaces between bone and two interbody cages of lumbar spine segments. *Spine*, 2001; 26(13):1437-42
- 8 White AA, Panjabi MM. *Clinical biomechanics of the spine* (2nd Edition). JB Lippincott Company, Philadelphia, 1990.

Figure Legends

Figure 1: Meshed Finite Element Geometry showing applied loads and boundary conditions

Figure 2: Predicted von Mises stresses (Pa) for benchmark finite element simulation

Figure 3: Predicted von Mises stresses (Pa) for implant contact surface

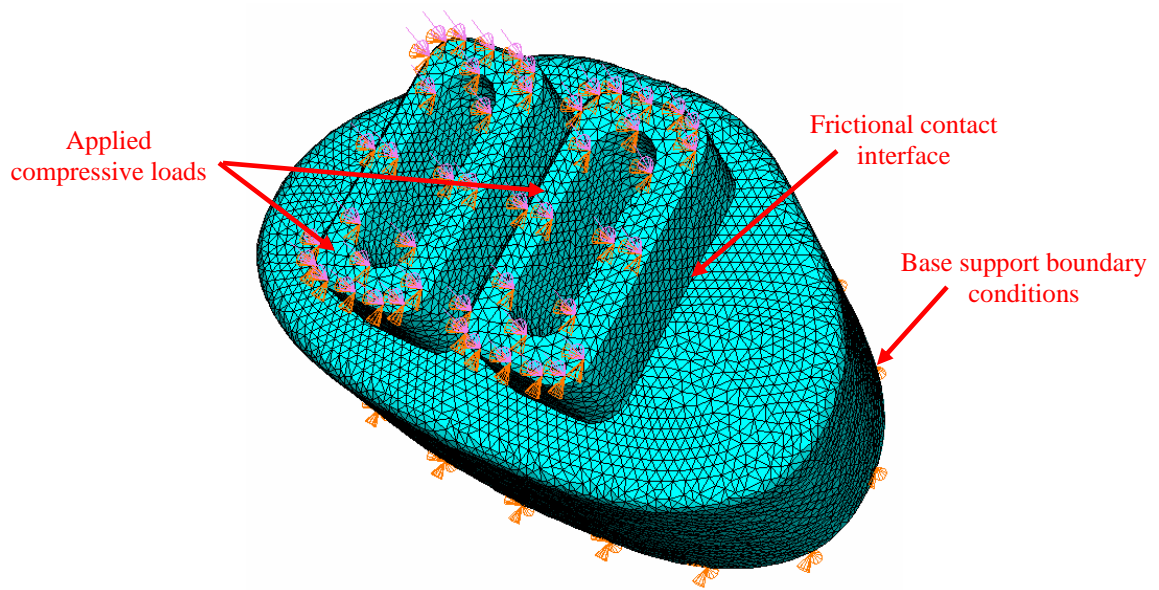
Figure 4: Predicted deformation profile of vertebral end plate (*one implant removed for visualisation purposes, deformations magnified 100 times*)

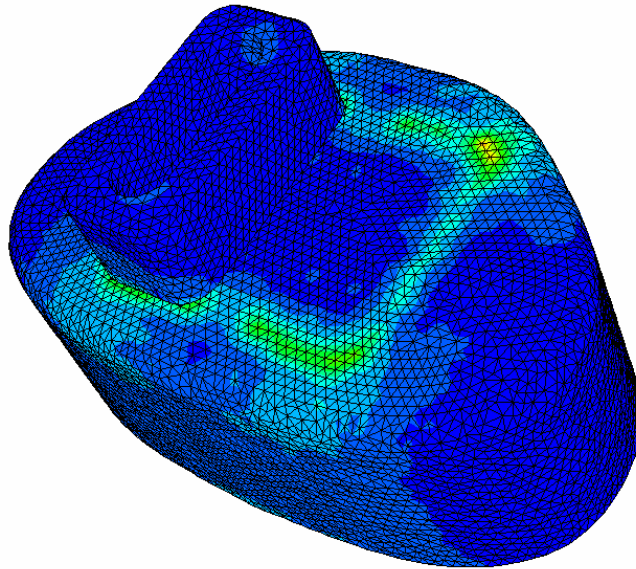
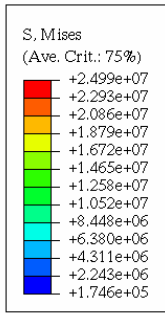
Figure 5: Variation of predicted maximum stresses in vertebral end plate with cancellous core elastic modulus

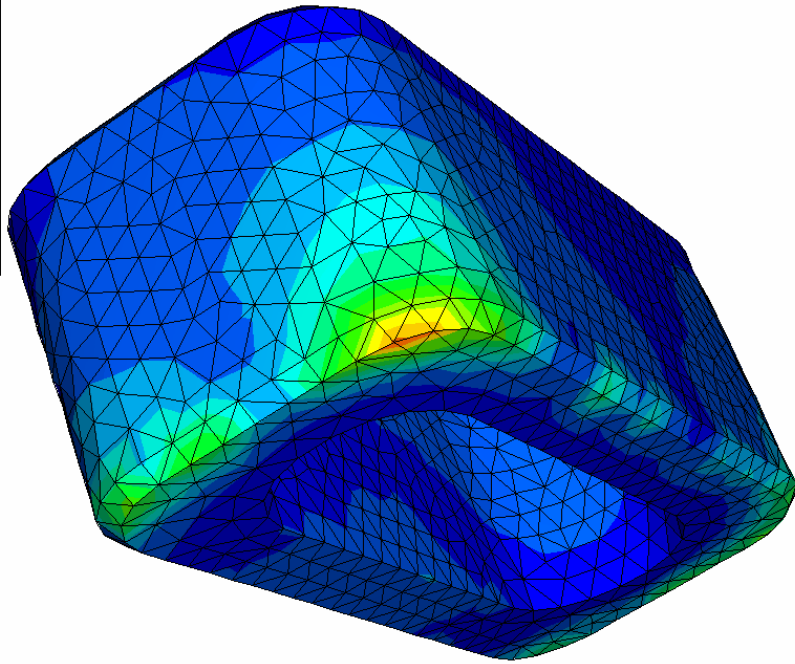
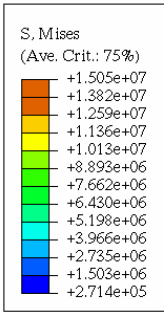
Figure 6: Percentage of total applied load transmitted through cancellous core versus elastic modulus of core

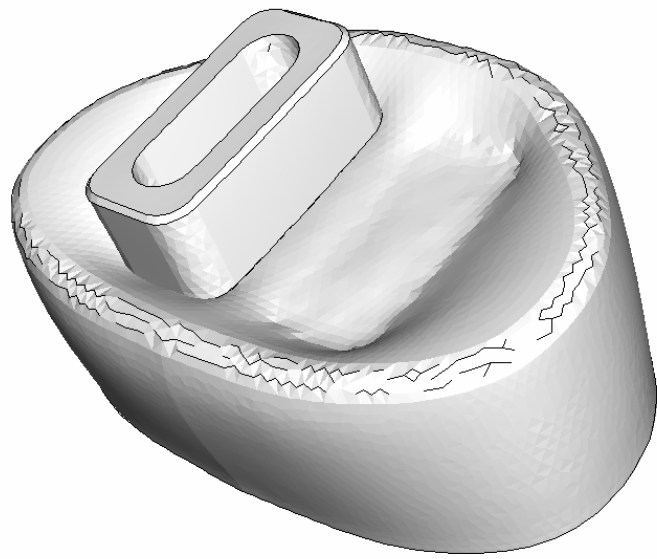
Figure 7: Maximum predicted von Mises stress versus elastic modulus of implant

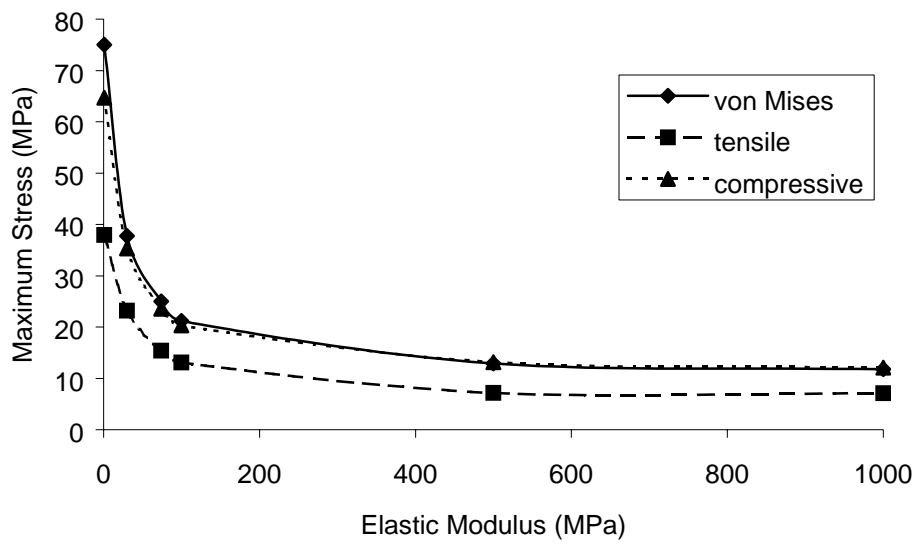
Figure 8: Beam bending analogy for implant and vertebral end plate

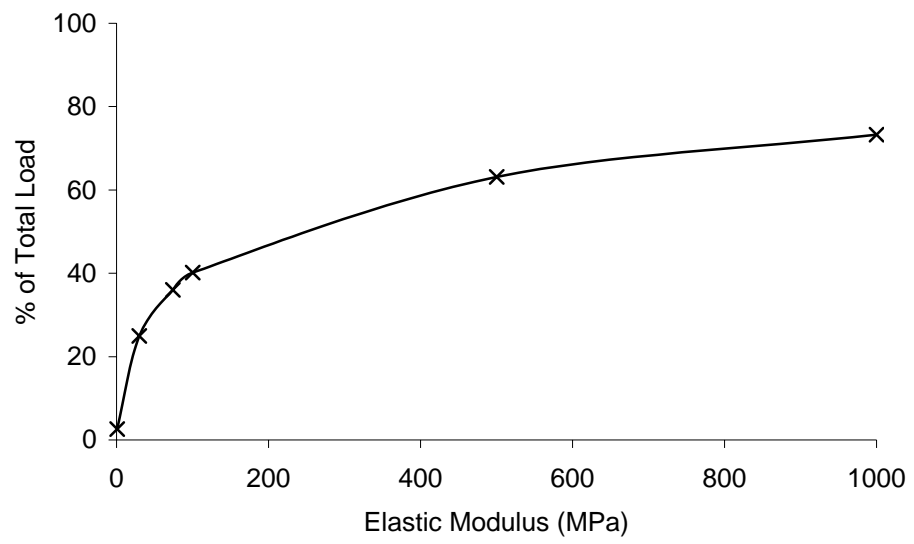


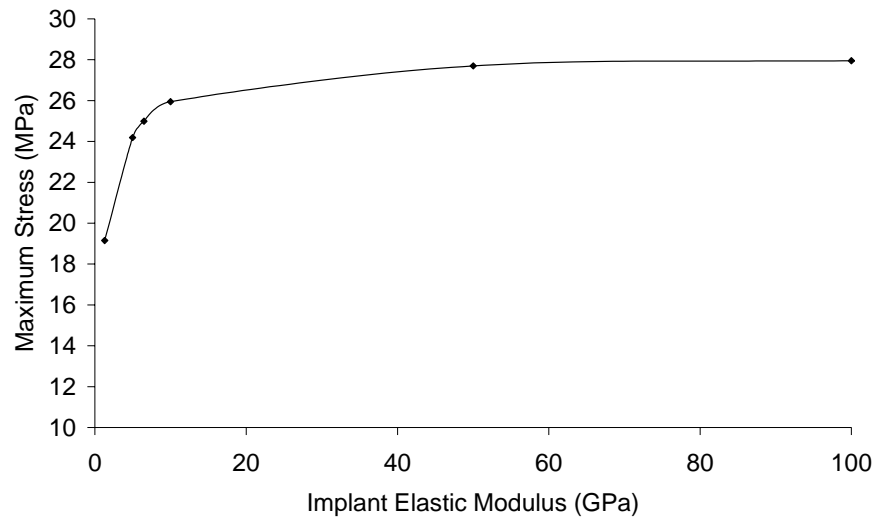












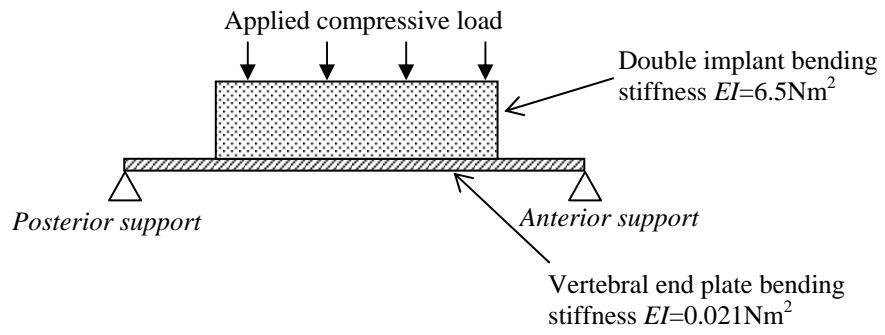


Table 1: Predicted Stress Levels for Benchmark Simulation

Parameter	Value
Applied load	610 N
'Nominal' contact stress	2.0 MPa
Maximum predicted contact stress	21.9 MPa
Maximum von Mises stress	25.0 MPa
Maximum tensile (principal) stress	15.4 MPa
Maximum compressive (principal) stress	23.6 MPa